Metallomics

Accepted Manuscript

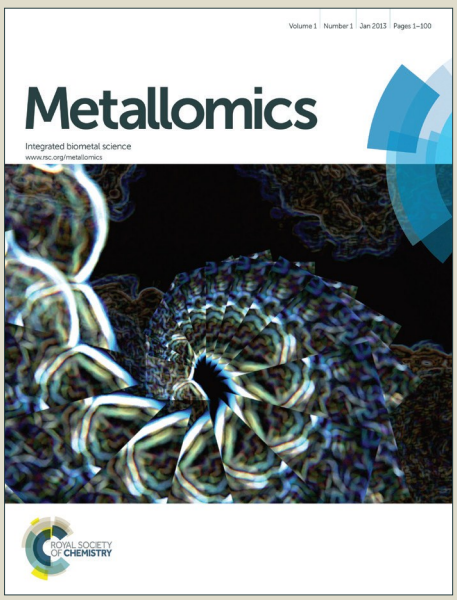

ROYAL SOCIETY OF CHEMISTRY

www.rsc.org/metallomics

Metallomics

RSCPublishing

ARTICLE

Cite this: DOI: 10.1039/x0xx00000x

Thermodynamics of Pb(II) and Zn(II) binding to MT-3, a neurologically important metallothionein

Received 00th January 2012,
Accepted 00th January 2012

DOI: 10.1039/x0xx00000x

www.rsc.org

M. C. Carpenter [a1], A. Shami Shah [b3], S. DeSilva [b4], A. Gleaton [b5], A. Su [b2], B. Goundie[b], M. L. Croteau [a], M. J. Stevenson [a], D. E. Wilcox [a*] and R. N. Austin [bc2*]

Isothermal titration calorimetry (ITC) was used to quantify the thermodynamics of Pb^{2+} and Zn^{2+} binding to metallothionein-3 (MT-3). Pb^{2+} binds to zinc-replete Zn_7MT-3 displacing each zinc ion with a similar change in free energy (ΔG) and enthalpy (ΔH). EDTA chelation measurements of Zn_7MT-3 and Pb_7MT-3 reveal that both metal ions are extracted in a tri-phasic process, indicating that they bind to the protein in three populations with different binding thermodynamics. Metal binding is entropically favoured, with an enthalpic penalty that reflects the enthalpic cost of cysteine deprotonation accompanying thiolate ligation of the metal ions. These data indicate that Pb^{2+} binding to both apo MT-3 and Zn_7MT-3 is thermodynamically favourable, and implicate MT-3 in neuronal lead biochemistry.

A. Introduction

Lead is a heavy metal whose distribution in the environment has been radically altered by human activities, yet it has no known beneficial function in biology.[1] Pb^{2+} substitutes primarily for Zn^{2+} and Ca^{2+} in biomolecules and exerts a wide range of toxic effects in all organisms in which its toxicity has been studied.[2] In humans, its effects can be separated into acute toxicities that are seen at relatively high doses, and pernicious effects on learning and behaviour that manifest at much lower doses and are most directly correlated with lead exposure in young children.[3, 4] Recent studies suggest that childhood lead exposure can be linked to central nervous system pathologies later in adulthood.[5-9]

Much is still unknown about mammalian transport of Pb^{2+}. It is thought to enter the body primarily through divalent metal transporters (DMTs),[10] and may cross the blood-brain barrier through passive diffusion as the $Pb(OH)^+$ ion.[11, 12] Given its high affinity for both thiol and carboxylate ligands, Pb^{2+} is likely to be associated with endogenous proteins inside the brain, but their identities are unclear.[13]

Metallothioneins (MTs) are potential mediators of Pb^{2+} biochemistry.[14-20] They are small (~60 residue) proteins with 20 cysteines that can bind a total of 7 divalent metal ions (normally zinc) and as many as 12 monovalent ions.[14-21] They have been considered "heavy metal sponges", protecting living organisms from the deleterious effects of toxic metals that induce their biosynthesis. Once expressed, they bind and sequester the inducing toxic metal ions.[22-24] More recent research has focused on whether MT buffers the concentration of Zn^{2+} for storage and delivery to its intended sites (a homeostasis function),[24-28] or whether it plays a role in protecting biological systems from oxidative stress by neutralizing reactive oxygen species (ROS) or reactive nitrogen species (RNS) through redox reactions of its Cys thiols.[29-35]

There are four common isoforms of mammalian metallothionein, MT-1, MT-2, MT-3 and MT-4, all of which are Class I members of the MT family of proteins.[36] MT-3 is primarily expressed in human brain tissue, which suggests it could have a potential role in modulating lead neurochemistry.[19, 37-39] This isoform binds metal ions with a typical MT structure consisting of two distinct metal-thiolate clusters, one in the C-terminal α domain and the other in the N-terminal β domain, which are separated by a short spacer.[40, 41] However, MT-3 has a conserved acidic hexapeptide insert near the C-terminus in the α domain and a unique pair of prolines (-TCPCPS-) near the N-terminus in the β domain, which may contribute to distinctive biochemical properties.[41]

MT-3 is frequently isolated as an air-stable mixed Cu^{+}/Zn^{2+} species but its levels are correlated with *in vivo* zinc concentrations, suggesting the potential for a key role in neuronal Zn/Cu-metallobiochemistry.[42-44]

The *in vivo* chemistry of MT-3 is less understood than that of the other MT isoforms.[14, 21, 37, 45] Also known as the neuronal "growth inhibitory factor" (GIF),[46-48] MT-3 may protect against certain brain pathologies.[49-51] Some studies have shown that MT-3 is present at lower concentrations in the brains of individuals with Alzheimer's disease (AD), relative to healthy counterparts,[52, 53] although other reports failed to confirm this result consistently.[21, 54] It is believed that MT-3 can ameliorate the toxicity of AD by chelating Cu^{2+} that is bound to $A\beta_{1-40}$,[37] based on the observation that MT-3 abolishes the production of ROS by $A\beta_{1-40}$, presumably by removing the redox-active metal ion.[37, 55]

The metal binding properties of MT have been examined with Zn^{2+}, Cd^{2+}, Hg^{2+}, Cu^{+}, Ag^{+}, Au^{+}, Fe^{2+}, Co^{2+}, Bi^{3+}, and As^{3+}.[44, 56-62] These studies have investigated both metal ion binding to the apo (metal free) protein and metal displacement from the protein, which provides a ranking of its metal affinity that reflects the thiophilicity of the metal ion. Metallation of the apo form of the protein occurs rapidly.[24, 63] CD spectroscopy indicates that apo MT is relatively unstructured in the absence of metal ions, which stabilize a well-defined protein structure upon binding.[64, 65] The role of partially structured forms of the protein during (de)metallation reactions is of current interest.[66]

Due to its high affinity for several thiophilic closed-shell metal ions and its susceptibility to oxidation, fewer studies have quantified metal binding by MT. Early studies used pH titrations[67-69] and electrochemical methods[68, 70] to determine average binding constants for Zn^{2+} and Cd^{2+}. Kretzel and Maret used competition with fluorescent ligands to show that four zinc ions bind to MT-2 with a binding constant of 6.3×10^{11}, and three additional zinc ions bind with weaker affinity (3.1×10^{10}, 7.9×10^{9}, and 5×10^{7}).[27] Recently, Pinter and Stillman have reported individual Zn^{2+} binding constants in the range 6.3×10^{11} to 3.2×10^{12} from mass spectrometry measurements.[71] An average binding constant of 6.2×10^{10} has been reported for Zn^{2+} binding to MT-3.[67]

Both qualitative and quantitative information on Pb^{2+} binding to MT is surprisingly sparse, in spite of numerous studies that have sought correlations between MT expression and lead exposure.[72-75] In 1984, Waalkes, *et al* demonstrated that 1.5 μM Pb^{2+} displaced 50% of the Zn^{2+} from 100 μg of rat hepatic Zn_7MT in 1 mL of solution.[62] Only Cd^{2+} was found to have a lower EC_{50}, but 5% of the zinc was still bound in the presence of 1 mM Pb^{2+}, which was a higher percentage than most other metals studied. Later studies have suggested that lead binds to metallothioneins more tightly than zinc[76,77], although with potentially complex kinetics.[78, 79]

The technique of isothermal titration calorimetry (ITC) is capable of measuring the thermodynamics of metal ions binding to peptides and proteins.[80-83] To date, ITC has not been widely used to study metal ions binding to MT, which is likely due to the oxygen sensitivity of the apo protein that hampers its characterization by ITC and other methods. This issue, however, can be addressed by performing ITC measurements under an inert atmosphere. Herein, we report the results from anaerobic ITC measurements of Pb^{2+} displacing Zn^{2+} from Zn_7MT-3 and experiments in which EDTA was used to chelate metal ions from both Pb_7MT-3 and Zn_7MT-3. These results provide important insight into Pb^{2+} binding to both the apo form of the protein and Zn_7MT-3.

B. Experimental Procedure

Materials and methods

MT-3 in the pGEX-4T1 (GE Healthcare, Little Chalfont, UK) was a generous gift of Professor Silvia Atrian, University of Barcelona and purified using a modified version of previously published protocols.[40, 58] An Akta UP10 FPLC was used for protein purification and a Coy chamber was used for anaerobic protein manipulations. Low speed centrifugation was done with a Sorvall RC-5C Plus centrifuge and higher speed centrifugation above 10,000 rpm were done with Beckman Optima LE-80 ultracentrifuge.

MES and bis-Tris buffers were purchased in highest purity from Sigma-Aldrich as were metal salts, dithiothreitol (DTT), and 5,5'-dithiobis-(2-nitrobenzoic acid) (DTNB). Thrombin from bovine plasma was obtained from GE Healthcare. HiTrap™desalting columns were purchased from GE healthcare. All buffers were prepared with nanopure (18 MΩ) water in acid washed glassware and treated for at least 1 hour with Chelex 100® cation exchange resin. The buffers were then filtered and ~200 mL volumes of buffer were degassed under vacuum with stirring until no air bubbles were seen, usually 0.5-1 hr. Degassed buffers were moved into a glovebox and sparged for 10 minutes with Ar. Metal and chelate stock solutions were prepared using the appropriate mass of metal salt or chelate solid, and then diluted with oxygen free buffers in the glovebox. The concentrations of metals in experimental solutions were verified by titrating metal solutions into EDTA in the ITC and ensuring that the result matched the stoichiometry, and the enthalpy, reported in the literature.

Protein Purification

Zn_7MT-3 was prepared by first transforming *E. coli* BL21 cells with the MT-3 pGEX-4T1 plasmid. Cells were grown overnight at 37 °C on LB agar containing 100 μg/mL ampicillin. A single colony from the LB plate was used to inoculate 250 mL of LB containing 100 μg/mL ampicillin. This culture was incubated at 37 °C and agitated at 200 rpm for 16 to 18 hours. 20 mL of the LB culture was added to a 2.8 L flask containing 400 mL of TB media with 100 μg/mL ampicillin, and then incubated at 37°C and 200 rpm. The optical density was monitored at 600 nm (OD_{600}) using a Beckman Coulter DU 800 spectrophotometer. Once OD_{600}

reached 0.7, 1 mM isopropyl β-D-1-thiogalactopyranoside (IPTG) was added to induce MT-3 expression. After incubation at 30 °C and 200 rpm for 1 h, 0.5 mM $ZnCl_2$ was added and the cultures were incubated at 37 °C and 200 rpm for 16-18 hours. The cells were then harvested by centrifugation at 8,000 rpm for 15 min, and stored at -80 °C. Alternatively, cells were grown using the BioSilta EnPresso B growth system following all of the manufacturer's instructions.

Cells were thawed, separated into approximately 15 g portions, and each portion was suspended in a solution of 1.248 g sucrose in 15 mL PBS (140 mM NaCl, 2.7 mM KCl, 10 mM Na_2HPO_4, 1.8 mM KH_2PO_4). Argon was bubbled through the mixture before centrifuging at 8,000 rpm for 15 min at 4 °C and collecting the pellets. The pellets were then resuspended in 15 mL PBS and 6 μL β-mercaptoethanol (BME), bubbled with argon, and centrifuged at 8,000 rpm for 15 min at 4 °C. The pellets were collected and resuspended in 10 mL PBS containing 1 mM DTT and 0.1 mM PMSF, and sonicated for one min at 30 W, 15 W and 8 W, with two min rest between sonications. The mixtures were then centrifuged at 8110 x g for 15 min at 4 °C. The supernatant was collected and centrifuged at 48,000 rpm for 30 min before being filtered through 0.22 μm syringe filter units. A Bradford Standard Assay using Bovine Serum Albumin (BSA) or a Nanodrop assay were used to determine the protein concentration of the cell lysate.

GST tagged MT-3 was isolated from the cell lysate using GE Healthcare GSTrap FF columns. The columns were prepared by washing with 5 column volumes (CV) of filtered and degassed nanopure water, followed by 5 CV of filtered and degassed PBS. Cell lysate was loaded onto the column, and the unbound sample was washed out with 10 CV of PBS. The MT-3 fusion protein was collected by flowing 2 CV of an elution buffer (50 mM Tris-HCl, 10 mM reduced glutathione, 2.5 mM DTT) through the column and collecting the output in 4 mL fractions. Appropriate fractions were combined and concentrated using 30 kDa Amicon centrifugal filter units. Bradford Standard Assays or protein determination on a Nanodrop were performed to determine protein concentration.

To cleave the fusion protein, bovine plasma thrombin was added to a concentration of 1 unit/100 μg of protein, and the sample was allowed to incubate overnight at room temperature while undergoing gentle agitation. The sample was then loaded onto a HiLoad 26/600 75pg size exclusion column, which had been previously calibrated with a protein calibration kit, and MT-3 was eluted with PBS. MT-3 typically eluted between 200 and 250 mL. These fractions were collected and concentrated in 3 kDa centrifugal filter units, and an aliquot was run on a 15% polyacrylamide SDS–PAGE gel with silver staining to confirm the presence of protein. To determine the MT-3 concentration, the absorbance of the samples in 0.1 M HCl was measured at 220 nm, and calculated using an extinction coefficient of 53,000 $M^{-1}cm^{-1}$.[45]

To demetallate MT-3, the pH was lowered to 3 by the addition of 1 M HCl. 1 mM dithiothreitol (DTT) was then added and the sample was loaded onto a HiTrap desalting column and eluted with 0.05 N HCl. The eluent was collected in 1 mL fractions, and the absorbance at 220 nm was used to determine which fractions contained MT-3. Those samples were buffer exchanged into water and lyophilized. Lyophilized MT-3 was resuspended in 1 mL of deoxygenated 100 mM MES (or bis-Tris), pH 6.0 and incubated with 80 mM DTT at ambient temperature for one hour under a nitrogen atmosphere. The protein was then passed down a desalting column equilibrated with 100 mM MES (or bis-Tris), pH 6.0. The concentration of MT-3 was determined both by using a DTNB assay to measure the concentration of free thiols (20 free thiols per protein) and by measuring the absorption at 220 nm in 0.1 M HCl as described above. The DTNB assay was performed by adding 20 μL of DTNB from a 5 mg/mL stock solution in pH 8 50 mM bis tris buffer and 80 μL of the peptide solution to 900 μL of 50 mM Tris, pH 8. The absorbance of the solution at 412 nm was measured within 10 minutes, and the concentration of free thiol in solution determined using ε_{412}=14,150 $cm^{-1}\bullet M^{-1}$.[1] To form M_7MT-3, 7 equivalents of $Pb(NO_3)_2$ or $ZnCl_2$ were added to the apo protein. All manipulations with the apo form of the protein were carried out in an anaerobic Coy Chamber. Given metallothionein's proclivity towards oxidation,[84] reduction and remetallation were done in a Coy Chamber immediately before each ITC experiment.

ITC data collection and analysis

For ITC experiments, the protein concentration was determined as described above. The concentration of the EDTA solution was 10 times the concentration of M^{2+} in the protein solution and prepared in the same buffer. For the displacement titrations, the concentration of $Pb(NO_3)_2$ was 10 times the concentration of Zn^{2+} in the Zn_7MT-3 samples and prepared in the same buffer. All experiments were performed on a MicroCal VP-ITC in a custom built glovebox that was continuously purged with N_2 prior to and during experiments, which were performed at 25 ± 0.2 °C and 307 rpm stirring. Titrant was normally delivered to the cell in 30-40, 8-10 μL injections. The heat of dilution, determined by the heat of the final injections of each experiment, was subtracted from the integrated data. The pH, concentrations and ionic strength of the buffers were always carefully matched between the titrant and cell solutions. The data are presented as the baseline-adjusted heat flow vs time in the upper panel, and the integrated concentration-normalized molar heat per injection vs the molar ratio of titrant to titrand in the lower panel. The data were analyzed using a one set of sites, two sets of sites, or competition binding model provided in Origin 7.0 software by MicroCal. All reported thermodynamic parameters are the average and standard deviation of at least two datasets. In order to accurately quantify the binding constant of the third inflection with the competition binding model, the concentration of the protein in the cell was adjusted so that the inflection of interest occurred at a 1:1 molar ratio, which had no effect on the value of the binding constant or

the binding enthalpy given by the fitting model. The competition binding model has a narrow 'window' of conditions for convergence to a unique and reasonable fit.[85] This required that the concentrations in the syringe and the cell, and therefore the input (fixed) binding enthalpies, be scaled by a factor of 10^3 for convergence to a unique binding constant.

C. Results and Analysis

Quantifying the affinity of a protein for metal ions *in vitro* provides critical information about its expected *in vivo* metal-binding properties. ITC, which measures the heat of binding, is a versatile method for determining metal binding constants. ITC experiments require a known concentration of the metal and the starting protein sample, and the accuracy of these values are independently confirmed by the stoichiometry from the fit of the titration data. ITC experiments can also quantify the metal-binding enthalpy, but the enthalpies of other coupled reactions (e.g., protonation, deprotonation) that contribute to the net enthalpy need to be subtracted to determine the desired metal coordination enthalpy.

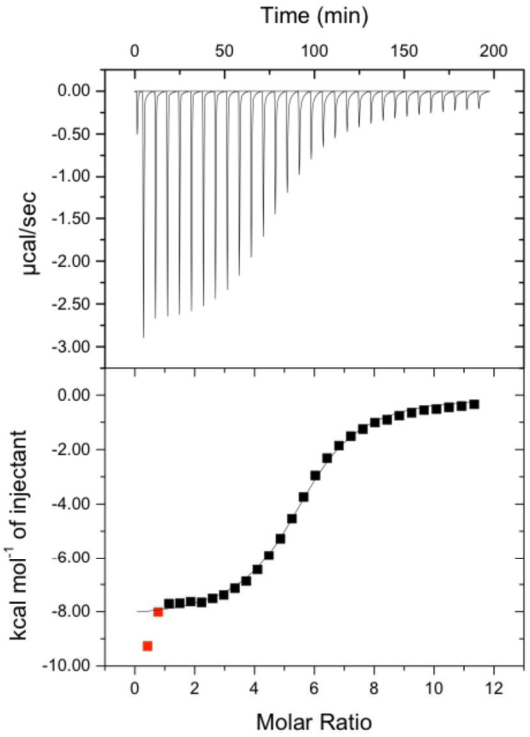

Figure 1. ITC measurement of Pb^{2+} titration into Zn_7MT-3 in MES buffer, pH 6.0; best-fit values are n_{ITC} = 5.8 +/- 0.03, K_{ITC} = 3.1 (+/- 0.2) x 10^5, ΔH_{ITC} = -7.16 +/- 0.05 kcal/mol.

The high cysteine content of MT provides a significant challenge to direct ITC measurements of metal ions binding to the apo protein. Therefore, two alternate measurements, metal displacement from the protein and metal chelation from the protein, were used to indirectly determine the MT-3 metal-binding thermodynamics. The latter provides the binding thermodynamics based on the principle of microscopic reversibility, after accounting for the metal-chelate binding thermodynamics, and has been used successfully in recent ITC studies where direct measurement of metal ions binding to a protein was not feasible.[82,86]

To quantify Pb^{2+} competition with the native Zn^{2+} for MT-3, ITC measurements of Pb^{2+} titrations into Zn_7MT-3 were used to determine the displacement thermodynamics, as indicated by the Scheme 1 equilibrium.

$$7\ Pb^{2+} + Zn_7MT\text{-}3 \rightleftharpoons Pb_7MT\text{-}3 + 7\ Zn^{2+}$$

Scheme 1

The thermograms that result from these titration have, as shown in a representative example in Figure 1, a single inflection that can be fit to a one-site binding model. The experimental values, averaged from two independent experiments, are n_{ITC} = 6.9 +/- 1.5, K_{ITC} = 3 x 10^5 and ΔH_{ITC} = -9 kcal/mol of Pb^{2+} for the displacement. These values were determined from the known concentration of the protein and the metal titrant, thus confirming the metal stoichiometry of Pb_7MT-3 at the end of the titration. The concentration and identity of the starting sample, Zn_7MT-3, was independently established prior to each titration, as the reduced apo form of the protein was prepared in an anaerobic chamber adjacent to the calorimeter, which was also housed in an anaerobic chamber, and both the concentration of free thiols and the concentration of the protein were determined. Seven equivalents of Zn^{2+} were then added to generate Zn_7MT-3.

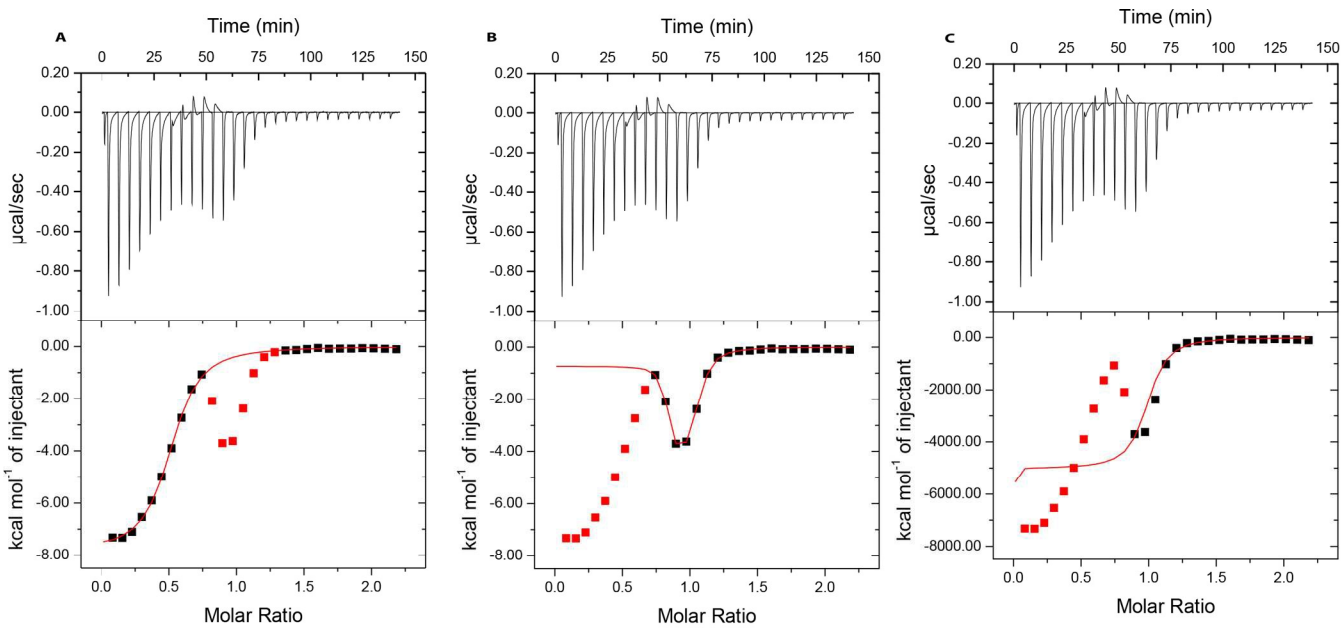

Figure 2 ITC measurement of EDTA addition to Pb_7MT-3 in 100 mM MES, pH 6.0; A) fit of first inflection with one-site model, n_{ITC} = 0.50 +/- 0.01, K_{ITC} = 8.3 (+/- 0.5) x 10^5, ΔH_{ITC} = -7.8 +/- 0.1 kcal/mol; B) fit of second and third inflections with two-sites model, n_{1ITC} = 0.80 +/- 0.01, K_{1ITC} = 3 (+/- 1) x 10^8, ΔH_{1ITC} = -0.7 +/- 0.1 kcal/mol, n_{2ITC} = 0.20 +/- 0.01, K_{2ITC} = 1.7 (+/- 0.2) x 10^6, ΔH_{2ITC} = -5.0 +/-0.03 kcal/mol; C) fit of third inflection with competition model, K_A = 1.3 x 10^{14} (fixed), ΔH_A = -1.1 x 10^4 kcal/mol (fixed), ΔH_B = -6.6 x 10^3 kcal/mol (fixed), K_{BITC} = 8 (+/- 2) x 10^{11}; red points were masked for fitting purposes.

To determine the thermodynamics of Pb^{2+} binding to MT-3, chelation titrations with EDTA were performed, as indicated by the Scheme 2 equilibrium.

$$7\ \text{EDTA} + \text{Pb}_7\text{MT-3} \rightleftharpoons \text{MT-3} + 7\ \text{PbEDTA}$$

Scheme 2

These titrations are unusual in that they have three inflections with alternating enthalpies, indicating the sequential removal of three populations of Pb^{2+} ions that are bound to MT-3 with unique thermodynamics (Figure 2). Because these data are complex, concatenated titrations in which the syringe was refilled with the titrant were performed. Data from the multiple files were then merged to create a single thermogram. The concentration of EDTA in the concatenated measurements was lowered to provide more injections and, therefore, more information about each chelation event (inflection) in the thermogram. The experimental stoichiometry of EDTA and the metallated protein at the titration endpoint confirms the metal occupancy of the starting protein sample.

To determine the Zn^{2+} binding thermodynamics, EDTA chelation of Zn^{2+} from MT-3 was measured with ITC, according to the Scheme 3 equilibrium.

$$7\ \text{EDTA} + \text{Zn}_7\text{MT-3} \rightleftharpoons \text{MT-3} + 7\ \text{ZnEDTA}$$

Scheme 3

Titration of EDTA into Zn_7MT-3 yielded isotherms with three inflections that are qualitatively similar to those of the Pb^{2+} chelation titrations, indicating that Zn^{2+} is also bound to MT-3 in three populations with different binding thermodynamics (Figure 3). Both the Pb^{2+} and Zn^{2+} chelation titrations required similar fitting and analysis to obtain the binding thermodynamic values. Again, the experimentally determined stoichiometry for the reaction between EDTA and the protein sample confirms the metal occupancy of the starting protein sample.

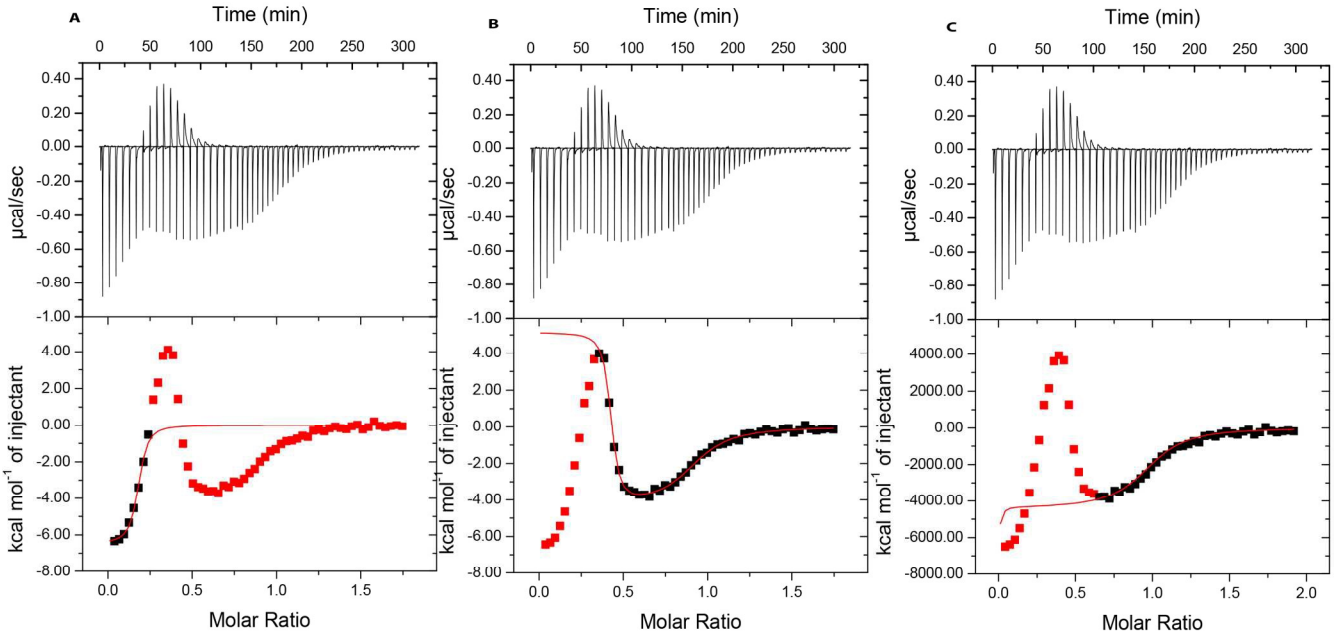

Figure 3. ITC measurement of EDTA addition to Zn_7MT-3 in 100 mM bis-Tris, pH 6.0; A) fit of first inflection with one-site model, n_{ITC} = 0.17 +/- 0.01, K_{ITC} = 2.3 (+/- 0.6) x 10^6, ΔH_{ITC} = -6.5 +/- 0.2 kcal/mol; B) fit of second and third inflections with two-sites model, n_{1ITC} = 0.41 +/- 0.01, K_{1ITC} = 1.3 (+/- 0.3) x 10^8, ΔH_{1ITC} = 5.14 +/- 0.03 kcal/mol, n_{2ITC} = 0.50 +/- 0.01, K_{2ITC} = 3.9 (+/- 0.5) x 10^5, ΔH_{2ITC} =-4.3 +/- 0.1 kcal/mol; C) fit of third inflection with competition model, K_A = 4.10 x 10^{12} (fixed), ΔH_A = -7.6 x 10^3 kcal/mol (fixed), ΔH_B = -3.2 x 10^3 kcal/mol (fixed), K_{BITC} = 7.8 (+/- 0.7) x 10^{10}; red points were masked for fitting purposes.

Because of the three inflections, which are sequentially exothermic, endothermic and exothermic, and a complicated stoichiometric relationship among MT-3, the metal ions, and the added chelate, none of the readily available models can fit the complete isotherm at once. In order to determine the net experimental enthalpy for each chelation event, only one or two inflections were fit at a time. For the concatenated data, it is possible to use the two-site binding model to separately fit the first and second inflections and the second and third inflections. The enthalpy value for the second inflection in both of these fits is equivalent, indicating that this piece-wise fitting approach is valid.

The experimental enthalpy values from the chelation experiments require additional analysis because of the multiple coupled equilibria upon addition of the EDTA. Specifically, ΔH_{ITC} includes dissociation of the metal ion from MT-3 (ΔH_{MT3-M}), the metal ion binding to EDTA (ΔH_{EDTA-M}) and displacing protons (ΔH_{EDTA-H}), and the concomitant protonation of the apo MT-3 (ΔH_{MT3-H}) and the buffer ($\Delta H_{buffer-H}$) (Scheme 4). Table 1 contains the three average experimental enthalpy values from the best fits of the Pb^{2+} and Zn^{2+} *chelation* measurements (columns a, b, c), and the correction for each metal binding to EDTA and displacing proton(s) that bind to the buffer at the experimental pH (column d; Supplementary Information), which is then used to determine the buffer-dependent enthalpies for the sequential *binding* of the three populations of metal ions to MT-3 (columns e, f, g). The experimentally determined stoichiometries of the three populations (columns h, i, j) then allow the weighted average buffer-dependent binding enthalpy per metal ion (column k) and the total buffer-dependent enthalpy for the formation of M_7MT-3 (column l) to be determined.

$$EDTAH^{3-} + H^+ \rightleftharpoons EDTAH_2^{2-} \quad \Delta H_{EDTAH2}$$

$$EDTA^{4-} + H^+ \rightleftharpoons EDTAH^{3-} \quad \Delta H_{EDTAH}$$

$$EDTA^{4-} + Zn^{2+} \rightleftharpoons ZnEDTA^{2-} \quad \Delta H_{ZnEDTA}$$

$$MT3^{n-} + Zn^{2+} \rightleftharpoons ZnMT3^{(n-+2)} \quad \Delta H_{ZnMT3}$$

$$MT3 + nH^+ \rightleftharpoons MT3H_n^{n+} \quad \Delta H_{MT3H}$$

$$buffer + H^+ \rightleftharpoons H^+buffer \quad \Delta H_{buffer}$$

Scheme 4 Equilibria that contribute to the experimental enthalpy measured in ITC chelation titrations.

The final values in Table 1 still include an enthalpy contribution from the protonation of buffer by protons that the metals displace from MT-3. Unfortunately, the number of protons that are displaced from the protein and bind to the buffer (n_{H+}) for each metal population (inflection) is not known. However, a comparison of these metal binding enthalpies to the enthalpy of Pb^{2+} displacing Zn^{2+}, which involves no protons but requires a correction for the difference between the metal-buffer interaction enthalpies (Table 1), reveals that 17 protons are displaced from MT-3 (n_{H+} = 17) when 7 metal ions bind to the apo protein at pH 6.0.

This information now allows us to determine the buffer-independent formation enthalpies for Pb_7MT-3 and Zn_7MT-3 (Table 2). Correcting for the protonation enthalpy of the buffer (column b), reveals a net endothermic formation of both metalloprotein complexes (column d). To compare the enthalpy of Pb^{2+} binding to MT-3 from these chelation measurements to the value determined from the displacement measurements, the deprotonation enthalpy of the MT-3 cysteines was estimated from the value for glutathione (column e). Accounting for the enthalpy from the displacement of 17 protons gives the enthalpy of 7 Pb^{2+} or 7 Zn^{2+} ions binding to fully deprotonated MT-3 (column f). The difference between these two values (-67 kcal/mol) is virtually identical to the experimental proton-independent enthalpy of 7 Pb^{2+} ions displacing 7 Zn^{2+} ions from MT-3 (-66 kcal/mol), which confirms the internal consistency of the displacement and chelation measurements.

Chelation titrations also allow the binding constants for the different populations of Pb^{2+} and Zn^{2+} ions to be determined. Because these titrations involve a competition between EDTA (species A) and MT-3 (species B), a competition model that can fit a single binding event was used to fit the third inflection.[82, 85] The binding constant (K_A) and binding enthalpy (ΔH_A) for Pb^{2+} or Zn^{2+} binding to EDTA under the experimental conditions (Supplementary Information), as well as the enthalpy for the third chelation event (ΔH_B) determined with other binding models (vide supra), were fixed parameters in these fits, which provided the K value for the third chelation event (K_B). Finally, K values for the first and second chelation events (inflections) were estimated from a comparison of the shape of the MT-3 isotherms to the bi-phasic chelation isotherms found with insulin (1 order of magnitude difference)[82] and OpdA (2.5 orders of magnitude difference).[86] We estimate that K values of the second and first chelation events are successively ~1.5 orders of magnitude smaller than K of the third chelation event. Since chelation is the reverse of binding, the average experimental values for each metal ion are indicated in Table 3 as the sequential binding constants, and binding free energies, for the three populations of metal ions binding to MT-3.

	a	b	c	d	e	f	g	h	i	j	k	l
					(-c+d)	(-b+d)	(-a+d)				(e*h+f*i + j*g)/7	(7*k)
Experiment		**ΔH_{ITC}**		**ΔH_{EDTA-M}**	**Buffer-Dependent enthalpy**			**Stoichiometry per population**			**ΔH_{MT3-M}**	**ΔH_{MT3-M}**
	Inflection 1	Inflection 2	Inflection 3		1st cations binding	2nd cations binding	3rd cations binding	1st cations binding	2nd cations binding	3rd cations binding	Weighted average per M^{2+}	Weighted average per MT-3
Pb^{2+} chelation	-6.7	0.5	-4.8	-10.6	-5.8	-11	-3.9	2.2	2.3	2.6	-7.0	-49
Zn^{2+} chelation	-6.5	5.7	-4.2	-7.6	-3.4	-13	-1.1	3.9	1.7	1.4	-5.4	-38
Experiment		**ΔH_{ITC}**		**$\Delta\Delta H_{buffer-M}$**					**$\Delta H_{displacement\ per\text{-}Pb^{2+}}$**		**$\Delta H_{displacement\ per\text{-}MT3}$**	
Displacement		-9		-0.5					-9.5		-66	

Table 1. Experimental enthalpies for chelation and displacement measurements of metal ions binding to MT-3 at pH 6.0, and analysis to obtain the buffer-dependent binding enthalpies; units of kcal/mol.

	a	b	c	d	e	f
				[a-(b*c)]		d+(c*e)
	Buffer-Dependent ΔH_{MT3-M}	**$\Delta H_{H-buffer}$**	**total H^+ displaced** (pH 6.0)	**Buffer-Independent ΔH_{MT3-M}**	**$\Delta H_{H\text{-}GSH}$**	**Deprotonated MT-3 thiols ΔH_{MT3-M}**
Pb^{2+} Binding	-49	-3.54	17	11.1	-8.5	-133
Zn^{2+} Binding	-38	-6.86	17	78.5	-8.5	-66
Displacement				-67		-67

Table 2. Analysis to determine the buffer-independent formation enthalpies for M_7MT-3 and the formation enthalpies with deprotonated Cys thiols; units of kcal/mol.

	population	# metals	# protons	K	ΔG^a	ΔH^a	$-T\Delta S^a$	ΔS^b
Pb^{2+}	1st	2.2	5.8	5.3×10^{11}	-16.0	+3.5	-19.5	65
	2nd	2.3	9.2	$\sim 1.6 \times 10^{10}$	-13.9	+3.2	-17.1	57
	3rd	2.6	2.0	$\sim 5 \times 10^{8}$	-11.9	-1.2	-10.7	36
Zn^{2+}	1st	3.9	12.6	6.8×10^{10}	-14.8	+18.8	-33.6	113
	2nd	1.7	4.4	$\sim 2.4 \times 10^{9}$	-12.8	+4.8	-17.6	59
	3rd	1.4	0	$\sim 7 \times 10^{7}$	-10.7	-1.1	-9.6	32

Table 3. Thermodynamic values from an analysis of calorimetric data for the three populations of metal ions binding to MT-3 at pH 6.0 and 298 K; a) units of kcal/mol, b) units of cal/mol K.

D. Discussion

Due to the difficulty of measuring the metal-binding thermodynamics of MT directly, two alternate experiments, chelation with EDTA and metal displacement, were used to quantify Pb^{2+} binding to MT-3. Recent success with the chelation of metal ions bound to insulin[82] and the binuclear metallohydrolase OpdA[86] guided these measurements. Analysis of the chelation data enables the change in free energy, enthalpy and entropy for metal ions binding to MT-3 to be determined without the complications of excess metal ions or oxidation of the apo protein. The formation enthalpies of both Pb_7MT-3 and Zn_7MT-3 have been determined by accounting for all coupled equilibria and determining the total number of protons displaced upon metal binding at the experimental pH (17 H^+). Accounting for the deprotonation enthalpy of the metal-binding Cys residues allows the metal displacement enthalpy to be estimated (-67 kcal/mol) from the Pb^{2+} and Zn^{2+} chelation enthalpies. The match between this estimated value and the experimentally measured displacement enthalpy (-66 kcal/mol) is remarkably good, indicating an internal consistency in the analysis of the binding thermodynamics.

The similar three-phase chelation isotherms for both Pb_7MT-3 and Zn_7MT-3 indicate that both metal ions bind to the protein in three populations with different thermodynamics. This is generally consistent with previous results for Zn^{2+} binding to MT-2,[27] where it was found that four Zn^{2+} bind with the highest affinity, two with a somewhat lower affinity and a 7th with even lower affinity. A complete thermodynamic analysis requires the number of protons displaced by each of the three populations of metal ions because protonation of the buffer upon metal binding to thiols contributes to the experimental enthalpy. Although we can determine the total number of protons displaced at pH 6.0 from a comparison of the enthalpy of the chelation data for both metal ions and the enthalpy of the displacement data that involves no proton displacement, careful deconvolution of chelation data in different buffers would be required to determine the number for each population. However, based on the known sequential (stochastic) metal-binding mechanism of MT and the coordination properties of these metal ions, we can estimate the proton displacement for each population and determine their individual binding thermodynamics. This analysis is based on the well-founded assumption that each metal ion will bind to four Cys and will displace the proton from each thiol if they are protonated (17 are protonated in apo MT-3 at pH 6.0). As indicated in Table 3, this allows us to estimate the number of protons displaced by each population of metal ions and thereby determine the buffer-independent binding enthalpy, and thus the binding entropy, for each population.

Metal Ion	Metallothionein	pH	*Apparent* Binding Constant(s)	Method	Ref
Zn^{2+}	Mammalian MTs	7.0	2×10^{12}		69
	MT-2	7.4	3.2×10^{13}	Cd NMR	87
	MT-2	7.5	1.3×10^{12}	DPP [c]	70
	MT-1	7.5	7.9×10^{11}	DPP [c]	70
	MT-2	8.0	3.1×10^{11}	^{19}F NMR w/5F-BAPTA	67
	MT-3	8.0	6.2×10^{10}	^{19}F NMR w/5F-BAPTA	67
	MT2a	7.4	6.3×10^{11} (4), 3.1×10^{10} (1), 7.9×10^{9} (1), 5×10^{7} (1)	UV-vis/Fluorescence	27
	MT-1 & MT-2	7.4	1.7×10^{11} (α domain), 1.8×10^{11} (β domain)	Fluorescence	88
	MT1a	7.0	3.3×10^{12}, 2.9×10^{12}, 2.3×10^{12}, 2.2×10^{12}, 1.6×10^{12}, 1.1×10^{12}, 6.3×10^{11}	ESI-MS	71
	MT-3	6.0	6.8×10^{10} (4), 2.4×10^{9} (~2), 7×10^{7} (~1)	ITC	this work
Cd^{2+}	Mammalian MTs	7.0	2×10^{16}		69
	Mammalian MTs	7.0 [a]	5×10^{15}	NMR	36
	MT-1	7.5	1.0×10^{15}	DPP [c]	70
	MT-2	7.5	6.3×10^{14}	DPP [c]	70
	Rabbit Liver MT		2.9×10^{10}		68
	MT-2	7.0[a]	7×10^{14}	Potentiometric titration	67
	MT-3	7.0 [a]	2×10^{14}	Potentiometric titration	67
Pb^{2+}	Mammalian MTs	7.0 [a]	2.5×10^{13}	Voltametry	36
	MT-2	4.7	5.3×10^{5}	ITC	76
	MT-3	6.0	5.3×10^{11} (~2), 1.6×10^{10} (~2), 5×10^{8} (~3)	ITC	this work
Cu^{+}	MT-1 [b] & MT-2 [b]	7.6	5.4×10^{19}	UV-vis w/CN^-	89
	MT-3 [b]	7.6	2.0×10^{21}, 2.6×10^{19}	UV-vis w/CN^-	89
	MT-2	7.5	4.1×10^{14}	ESI-MS	90

Table 4. Summary of the reported MT metal binding constants; for entries where multiple binding constants were reported, the number of metal ions that bind with each affinity is denoted in parentheses; a) values extrapolated to the denoted pH; b) mollusc MT c) differential pulse polography

The binding constants for the three binding events were determined by carefully fitting the data and by knowing the stability constant of the M^{2+}-EDTA product. The thermodynamics of Zn^{2+} binding to MT-3 largely reflect coordination to the Cys thiols, as found for Zn^{2+} binding to zinc fingers[91, 92] and small thiol-rich peptides.[93] There is an enthalpic penalty for removing the proton from cysteine, yet a more favorable entropic contribution from the loss and hydration of the displaced proton. The first population of ~4 Zn^{2+} ions that are bound most tightly to MT-3 each bind to four Cys thiols, most of which are protonated. The next population binds less tightly to the remaining free thiols and some that are already thiolates coordinating Zn^{2+} ions. The final population binds least tightly with exclusively weaker bridging thiolate coordination. As expected, the binding constants for Pb^{2+} binding to MT-3 are larger than those of Zn^{2+}, although not as large as predicted from the displacement measurements. The stoichiometries of the three metal populations are different for Pb^{2+} and Zn^{2+}. This likely reflects the larger size of the Pb^{2+} ion and its different coordination preference,[94] which is influenced by the stereochemical contributions of a lone pair of electrons.[95] Nevertheless, for both Pb^{2+} and Zn^{2+}, metal binding to protonated MT-3 is driven by the entropically favorable, yet enthalpically unfavorable, binding to the Cys thiols that are deprotonated upon coordination to dipositive metal ions.

The displacement titration data can be fit to a one-site binding model, suggesting that the difference between Pb^{2+} and Zn^{2+} in their binding free energies and binding enthalpies is nearly the same for all seven ions. This appears to reflect the intrinsic chemical properties of these two metal ions when coordinated to thiolates and not their specific coordination to MT-3, as the displacement thermodynamics is the same for the first and last Zn^{2+}, with no difference among the three populations of bound Zn^{2+} ions. While a careful analysis of the binding enthalpies from the chelation and displacement measurements shows an internally consistent value (vide supra), the displacement equilibrium constant ($K \sim 10^5$) is larger than predicted with the stability constants from the chelation data ($K_{Pb} \sim 10 \times K_{Zn}$ for each population; Table 3). From the chelation experiment data, it is possible to calculate an overall β_7 using the K values in Table 3 and weighting them by the number of metal ions in each population. This analysis yields $\beta_7 = 7.6 \times 10^{71}$ for Pb^{2+} binding to apo MT-3 and $\beta_7 = 1.5 \times 10^{69}$ for Zn^{2+} binding to apo MT-3. An alternate interpretation of the displacement titration is a cooperative process in which the addition of one equivalent of Pb^{2+} leads to $1/7^{th}$ equivalent of Pb_7MT-3. If this is the case, then the equilibrium constant for the displacement reaction is determined by the ratio of the two β_7 values, which is 500 and still smaller than the experimental displacement value ($\sim 10^5$).

A difference between the formation of Pb_7MT-3 by Pb^{2+} binding to apo MT-3 and by Zn^{2+} binding to apo MT-3 followed by Pb^{2+} displacement, as illustrated by the thermodynamic cycle in Figure 4, is the presence of displaced Zn^{2+} ions in the latter. These may contribute to a more stable Pb_7MT-3 structure, perhaps consistent with a report that MT-3 has an 8^{th} binding site for metal ions,[45] or other reports that MT can bind "excess" metal ions forming super-metallated complexes.[24, 79] In contrast, both the Pb^{2+} and Zn^{2+} EDTA chelation experiments start from the canonical form with seven metal ions and thus avoid complications from the presence of excess metal ions. The seventh root of the β_7 value gives the average K value for the seven metal ions binding to MT-3. This value is 1.9×10^{10} for Pb^{2+} and 7.6×10^9 for Zn^{2+}.

The discrepancy between the equilibrium constant for the displacement reaction and the comparable value determined from the chelation experiments may reflect the free energy of protein folding, which can be considered a thermodynamic step that is distinct from the free energy of metal binding. Gibney *et al* illustrated this point when they engineered proteins with pre-form zinc binding sites.[93] Comparing metal binding to proteins with pre-formed sites to metal binding to similar proteins that are not pre-folded enabled them to estimate the free energy of folding (positive) and the free energy of metal binding (negative). If the structures of Pb_7MT-3 and Zn_7MT-3 are different, as they may well be, then the free energy of protein folding may be different as well. Experiments are underway to probe this hypothesis further.

Four other studies have reported Pb^{2+} binding to metallothionein,[36 76, 77, 79] and several notable comparisons can be made with our results. Chu *et al* report an equilibrium constant for the displacement of Zn^{2+} by Pb^{2+} at pH 4.7 that is very similar to the value we find at pH 6.0 (1.3×10^5 vs 3×10^5), which is consistent with a minimal effect of pH on this process.[76] The binding constant of 5.3×10^5 that they report for Pb^{2+} binding to apo MT-2 at pH 4.7 is, unsurprisingly, considerably lower than the value determined from our chelation measurements at pH 6.0. While there is no evidence for triphasic binding under the more acidic conditions, they do report different structures for Pb_7MT formed by displacement of Zn^{2+} from Zn_7MT and Pb_7MT formed by titration of Pb^{2+} into apo MT, consistent with the different equilibrium constants we find for these two experiments. He *et al* also suggest structurally distinct forms of Pb_7MT as a function of pH.[77] Palacios *et al* report that addition of seven equivalents of Pb^{2+} initially results in the displacement of some Zn^{2+} from Zn_7MT-1, creating mixed metal species, but that Zn^{2+} re-displaces Pb^{2+} over 48 hours,.[79] The time scale of this reported re-equilibration, however, is considerably longer than our ITC measurements. Thus, the results of Chu *et al*[76], Kagi *et al*[36] and He *et al*[77] and the results reported here are all consistent with a predominant Pb_7MT species formed, at least initially, upon addition of seven equivalents of Pb^{2+} to either Zn_7MT or apo MT.

Table 4 places our results in the context of other published binding constants for zinc, cadmium, lead and copper binding to mammalian metallothionein. Two important trends are notable. First, the metal binding affinities follow the expected trend $Zn^{2+} < Pb^{2+} < Cd^{2+} < Cu^{+}$. Experimental results presented here for MT-3 confirm that it has a higher affinity for Pb^{2+} than it does for Zn^{2+}, and that the toxic metal ion readily displaces biologically-relevant Zn^{2+} from MT-3. Second, while certain methods are only capable of determining an average affinity for the several metal ions that bind to MT, other methods, including ITC used here, are able to quantitatively distinguish different affinities for metal ions binding to MT. This has been shown previously for MT-1 and MT-2, and our results demonstrate that Zn^{2+} binds to MT-3 in three sets with different affinities and binding thermodynamics. This study has also shown that Pb^{2+} similarly binds to MT-3 in three sequential sets, each with a higher affinity than the corresponding set of Zn^{2+} ions. The binding constants we find for Zn^{2+} can be compared to the reported values for other mammalian MT's. The K values for the three MT-3 populations at pH 6 are somewhat lower than the corresponding values reported previously for MT-2 at pH 7.4 [27] The average MT-3 affinity for Zn^{2+} found here (7.6×10^9) is also a little lower than the reported value for MT-3 at pH 8 (6.2×10^{10}).[67]

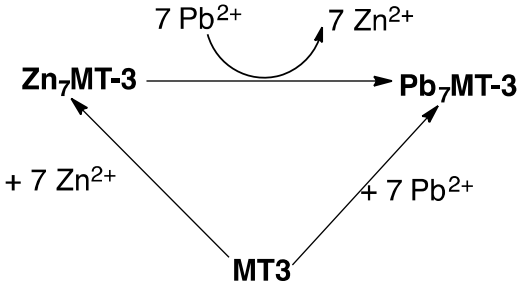

Figure 4. Thermodynamic cycle showing Zn^{2+} or Pb^{2+} ions binding to apo MT-3, and the displacement of Zn^{2+} from Zn_7MT-3 by Pb^{2+} to form Pb_7MT-3.

These *in vitro* results provide new insight about the *in vivo* neurochemical roles of MT-3 by delineating its physiologically relevant metal-binding properties. This study has shown that lead ions can outcompete zinc ions for binding to MT-3. It has also shown that zinc ions are bound to MT-3 with different affinities, consistent with the notion that zinc-replete MT-3 could donate some of its zinc ions to other biomolecules.

Conclusions

The results presented here confirm that MT-3 binds Pb^{2+} with a higher affinity than it does Zn^{2+} and that Pb^{2+} displaces bound Zn^{2+} ions. Competition experiments between the metal chelator EDTA and the metal-bound forms of MT-3 reveal a multiphasic extraction and therefore, based on microscopic reversibility, multiphasic binding. This likely reflects an initial higher affinity for coordination to terminal thiols followed by weaker coordination to bridging thiolates, but may include protein rearrangements during formation of the metal-protein complex, and is consistent with other reports of MT binding seven metal ions with different affinities. There are also intriguing parallels between the triphasic binding thermodynamics reported here and triphasic rates of metal ions binding to MT.[96]

The molecular mechanisms of lead neurotoxicity remain poorly understood. Given the limited solubility of Pb^{2+} under physiological conditions, and its strong affinity for thiol ligands, it is reasonable to presume that "free" Pb^{2+} ions are not found in the brain.[2, 97] However, the identity and nature of any chelator molecules is not known. This work shows that Pb^{2+} binding to both apo MT-3 and Zn_7MT-3 is thermodynamically favourable and thus MT-3 is a candidate protein to bind lead ions that cross the blood-brain barrier. It is not clear, though, whether Pb^{2+} binding to MT-3 would be a detoxification or merely serve as a short-term repository from which lead could be released under periods of oxidative stress.[98] Further studies to clarify the conditions under which Pb^{2+} is released from MT-3 and transferred to other potential neurological or pharmacological targets are underway.[26, 30, 37, 96, 99, 100]

1 Current address: Department of Chemistry and Biochemistry, University of Colorado, Boulder CO.
2 Current address: Department of Chemistry, Barnard College of Columbia University, New York NY 10027.
3 Current address: Department of Chemical Biology, Cornell University, Ithaca NY 14853
4 Current address: Boston Children's Hospital, Boston MA 02115
5 Current address: Tufts Medical School, Boston MA 02111

Acknowledgements

RNA acknowledges the NSF (CHE-1151957) and DEW acknowledges the NSF (CHE-1308598) for funding this research. Earlier funding was provided to Bates College by an Institutional Development Award from the NIGMS, grant number P20GM0103423. Earlier work on the project was carried out by Jess Howard, Rachel Carlson, Alex Stevenson, Hilary Ginsburg, Lesley Mo, and Kimberly Russell, whose contributions are gratefully acknowledged. Fruitful conversations with Ged Parkin, Columbia University, are also acknowledged.

Notes and references

[a] Department of Chemistry, Dartmouth College, Hanover NH, USA.
[b] Department of Chemistry, Bates College, Lewiston ME USA.
[c] Department of Chemistry, Barnard College, Columbia University, NY NY USA.
* To whom correspondence should be addressed dwilcox@dartmouth.edu or raustin@barnard.edu.
Electronic Supplementary Information (ESI) available: [procedure for determining K and ΔH for the formation of a M-EDTA complex]. See DOI: 10.1039/b000000x/

1. J. J. R. Frausto da Silva and R. J. P. Williams, *The Biological Chemistry of the Elements: The Inorganic Chemistry of Life*, Claredon Press, Oxford, 1991.
2. H. A. Godwin, The biological chemistry of lead, *Curr Opin. Chem Biol*, 2001, **5**, 223-227.
3. L. Patrick, Lead toxicity, a review of the literature. Part 1: Exposure, evaluation, and treatment, *Altern. Med. Rev.*, 2006, **11**, 2-22.
4. R. A. Goyer, Results of Lead Research: Prenatal Exposure and Neurological Consequences, *Environ. Health Persp.*, 1996, **104**, 1050-1054.
5. K. M. Bakulski, L. S. Rozek, D. C. Dolinoy, H. L. Paulson and H. Hu, Alzheimer's disease and environmental exposure to lead: The epidemiologic evidence and potential role of epigenetics., *Curr. Alzheimer Res.*, 2012, **9**, 563-573.
6. M. G. Weisskopf, Association of Cumulative Lead Exposure with Parkinson's Disease, *Environ. Health Persp.*, 2010, **118**, 1609-1613.
7. S. S. Coon, A., E. Peterson, A. Gloi, G. Kortsha, J. Pounds, D. Chettle and J. Gorell, Whole-Body Lifetime Occupational Lead Exposure And Risk Of Parkinson's Disease, *Environ Health Perspect.,* 2006, **114**, 1872-1876.
8. M. G. A. Opler, A. S. Brown, J. Graziano, M. Desai, W. Zheng, C. Schaefer, P. Factor-Litvak and E. S. Susser, Prenatal lead exposure, δ-aminolevulinic acid, and schizophrenia., *Environ. Health Persp.*, 2004, **112**, 548-552.
9. T. R. Guilarte, M. Opler and M. Pletnikov, Is lead exposure in early life an environmental risk factor for Schizophrenia? Neurobiological connections and testable hypotheses, *Neurotoxicology*, 2012, **33**, 560-574.

10. J. P. Bressler, L. Olivi, J. H. Cheong, Y. Kim and D. Bannona, Divalent metal transporter 1 in lead and cadmium transport, *Ann N Y Acad. Sci*, 2004, **1012**, 142-152.
11. M. W. Bradbury and R. Deane, Permeability of the blood-brain barrier to lead, *NeuroToxicology*, 1993, **14**, 131-136.
12. W. Zheng, M. Aschner and J.-F. Ghersi-Egea, Brain barrier systems: a new frontier in metal neurotoxicological research, *Toxicology and Applied Pharmacology*, 2003, **192**, 1-11.
13. B. Quintanilla-Vega, D. R. Smith, M. W. Kahng, J. M. Hernandez, A. Albores and B. A. Fowler, Lead-binding proteins in brain tissue of environmentally lead-exposed humans, *Chemico-Biological Interactions*, 1995, **98**, 193-209.
14. G. Meloni and M. Vasak, Redox activity of alpha-synuclein-Cu is silenced by Zn7-metallothionein-3, *Free Radical Bio Med*, 2011, **50**, 1471-1479.
15. M. Knipp, G. Meloni, B. Roschitski and M. Vasak, Zn7Metallothionein-3 and the Synaptic Vesicle Cycle: Interaction of Metallothionein-3 with the Small GTPase Rab3A, *Biochemistry*, 2005, **44**, 3159-3165.
16. E. Peroza and E. Freisinger, Metal ion binding properties of *Triticum aestivum* Ec-1 metallothionein: evidence supporting two separate metal thiolate clusters, *J. Biol. Inorg. Chem.*, 2007, **12**, 377-391.
17. H.-J. Hartmann and U. Weser, in *Biological Inorganic Chemistry*, ed. I. G. Bertini, Harry B.; Stiefel, Edward I.; Valentine, Joan Selverstone, University Science Books, Sausalito, 2007, pp. 156-174.
18. S.-J. Lee and J.-Y. Koh, Roles of zinc and metallothionein-3 in oxidative stress-induced lysosomal dysfunction, cell death, and autophagy in neurons and astrocytes, *Molecular Brain*, 2010, **3**, 30:(31-39).
19. C. Howells, A. K. West and R. S. Chung, Neuronal growth-inhibitory factor (metallothionein-3): evaluation of the biological function of growth-inhibitory factor in the injured and neurodegenerative brain, *FEBS Journal*, 2010, **277**, 2931-2939.
20. R. D. Palmiter, The elusive function of metallothioneins, *Proc. Nat. Acad. Sci. USA*, 1998, **95**, 8428-8430.
21. A. West, J. Hidalgo, D. Eddins, E. D. Levin and M. Aschner, Metallothionein in the central nervous system: roles in protection, regeneration and cognition, *NeuroToxicology*, 2008, **29**, 489-503.
22. C. A. Blindauer and O. L. Leszczyszyn, Metallothioneins: unparalleled diversity in structures and functions for metal ion homeostasis and more, *Nat. Prod. Rep.*, 2010, **27**, 720-741.
23. G. Roesijadi, Metal transfer as a mechanism for metallothionein-mediated metal detoxification, *Cell. Mol. Life Sci.*, 2000, **46**, 393-405.
24. D. E. K. Sutherland and M. J. Stillman, The "magic numbers" of metallothionein, *Metallomics*, 2011, **3**, 444-463.
25. A. Krezel and W. Maret, Thionein/metallothionein control Zn(II) availability and the activity of enzymes, *J. Biol. Inorg. Chem.*, 2008, **13**, 401-409.
26. W. Feng, J. Cai, W. M. Pierce, R. B. Franklin, W. Maret, F. W. Benz and Y. J. Kang, Metallothionein transfers zinc to mitochondrial aconitase through a direct interaction in mouse hearts, *Biochem Bioph. Res. Co.*, 2005, **332**, 853-858.
27. A. Krezel and W. Maret, Dual nanomolar and picomolar Zn(II) binding properties of metallothionein, *J. Am. Chem. Soc.*, 2007, **129**, 10911-10921.
28. M. Capdevila, R. Bofill, O. Palacios and S. Atrian, State-of-the-art of metallothioneins at the beginning of the 21st century, *Coord. Chem. Rev.*, 2012, **256**, 46-62.
29. Y. Li and W. Maret, Human metallothionen metallomics, *J. Anal. At. Spectrom.*, 2008, **23**, 1055-1062.
30. Y. Chen, Y. Irie, W. M. Keung and W. Maret, S-nitrosothiols react preferentially with zinc thiolate clusters of metallothionein III through transnitrosation, *Biochemistry*, 2002, **41**, 8360-8367.
31. W. Maret and B. L. Vallee, Thiolate ligands in metallothionein confer redox activity on zinc clusters, *Proc. Natl. Acad. Sci. USA*, 1998, **95**, 3478-3482.
32. R. Kassim, C. Ramseyer and M. Enescu, Oxidation reactivity of zinc-cysteine clusters in metallothionein, *J. Biol. Inorg. Chem.*, 2013, **18**, 333-342.
33. W. Maret, Metallothionein/Disulfide Interactions, Oxidative Stress, and the Mobilization of Cellular Zinc, *Neurochem. Int.*, 1995, **27**, 111-117.
34. Y. J. Kang, Metallothionein redox cycle and function, *Experimental Biology and Medicine*, 2006, **231**, 1459-1467.
35. W. Maret, Oxidative metal release from metallothionein via zinc-thiol/disulfide interchange, *Proc. Nat. Acad. Sci. USA*, 1994, **91**, 237-241.
36. J. H. Kagi and A. Schaffer, Biochemistry of metallothionein, *Biochemistry*, 1988, **27**, 8509-8515.
37. G. Meloni, V. Sonois, T. Delaine, L. Guilloreau, A. Gillet, J. Teissie, P. Faller and M. Vasak, Metal swap between Zn7-metallothionein-3 and amyloid beta-Cu protects against amyloid-beta toxicity, *Nature Chemical Biology*, 2008, **4**, 366-372.
38. J. Hidalgo and J. Carrasco, Regulation of the Synthesis of Brain Metallothioneins, *NeuroToxicology*, 1998, **19**, 661-668.
39. S.-J. Lee, K.-S. Cho, H. N. Kim, H.-J. JKim and J.-Y. Koh, Role of Zinc Metallothionein-3 (ZnMt3) in Epidermal Growth Factor (EGF)-induced c-Abl Protein Activation and Actin Polymerization in Cultured Astrocytes, *J. Biol. Chem.*, 2011, **286**, 40847-40856.
40. M. Capdevila, N. Cols, N. Romero-Isart, R. Gonzales-Duarte, S. Atrian and P. Gonzales-Duarte, Recombinant synthesis of mouse Zn3-beta and Zn4 alpha metallothionein 1 domains and characterization of their cadmium (II) binding capacity, *Cell. Mol. Life Sci.*, 1997, **53**, 681-688.
41. G. Oz, K. Zangger and I. M. Armitage, Three-dimensional structure and dynamics of a brain specific growth inhibitory factor: metallothionein-3, *Biochemistry*, 2001, **40**, 11433-11441.
42. R. Bofill, M. Capdevila and S. Atrian, Independent metal-binding features of recombinant metallothioneins convergently draw a step gradation between Zn- and Cu-thioneins, *Metallomics*, 2009, **1**, 229-234.
43. P. Faller, D. W. Hasler, O. Zerbe, S. Klauser, D. R. Winge and M. Vasak, Evidence for a dynamic structure of human neuronal growth inhibitory factor and for major rearrangements of its metal-thiolate clusters, *Biochemistry*, 1999, **38**, 10158-10167.
44. P. Palumaa, I. Tammiste, K. Kruusel, L. Kangur, H. Jornvall and R. Sillard, Metal binding of metallothionein-3 versus metallothionein-2: lower affinity and higher plasticity, *Biochem. Biophys. Acta.*, 2005, **1747**, 205-211.
45. G. Meloni, T. Polanski, O. Braun and M. Vasak, Effects of Zn(II), Ca(II), and Mg(II) on the structure of Zn7metallothionein-3: Evidence for an additional zinc binding site, *Biochemistry*, 2009, **48**, 5700-5707.
46. Z.-C. Ding, F.-Y. Ni and Z.-X. Huang, Neuronal growth-inhibitory factor (metallothionein-3): structure-function relationships, *FEBS Journal*, 2010, **277**, 2912-2920.
47. Z.-C. Ding, X.-C. Teng, B. Cai, H. Wang, Q. Zheng, Y. Wang, G.-M. Zhou, M.-J. Zhang, H.-M. Wu, H.-Z. Sun and Z.-X. Huang, Mutation at Glu23 eliminates the neuron growth inhibitory activity of human metallothionein-3, *BBRC*, 2006, **349**, 674-682.
48. A. K. Sewell, L. T. Jensen, J. C. Erickson, R. D. Palmiter and D. R. Winge, Bioactivity of Metallothionein-3 Correlates with its Novel beta Domain Sequence Rather than Metal Binding Properties, *Biochemistry*, 1995, **34**, 4740-4747.
49. Y. Manso, J. Carrasco, G. Comes, G. Meloni, P. A. Adlard, A. I. Bush, M. Vasak and J. Hidalgo, Characterization of the role of metallonthionein-3 in an animal model of Alzheimer's disease, *Cell. Mol. Life Sci.*, 2012, **69**, 3683-3700.
50. J. C. Erickson, G. Hollopeter, S. A. Thomas, G. J. Froelick and R. D. Palmiter, Disruption of the Metallothionein-III gene in Mice: Analysis of Brain Zinc, Behavior, and Neuron Vulnerability to Metals, Aging, and Seizures, *J. Neurosci*, 1997, **17**, 1271-1281.
51. Y. Manso, J. Carrasco, G. Comes, G. Meloni, P. Adlard, A. Bush, M. Vašák and J. Hidalgo, Characterization of the role of metallothionein-3 in an animal model of Alzheimer's disease, *Cell. Mol. Life Sci.*, 2012, **69**, 3683-3700.
52. Y. Uchida, K. Takio, K. Titani, Y. Ihara and M. Tomonaga, The growth inhibitory factor that is deficient in the Alzheimer's disease brain is a 68 amino acid metallothionein-like protein, *Neuron*, 1991, **7**, 337-347.

53. W. H. Yu, W. J. Lukiw, C. Bergeron, H. B. Niznik and P. E. Fraser, Metallotheinein III is reduced in Alzheimer's disease, *Brain Research*, 2001, **894**, 37-45.
54. J. Hidalgo, M. Aschner, P. Zatta and M. Vasak, Roles of the metallothionein family of proteins in the central nervous system, *Brain Research Bulletin*, 2001, **55**, 133-145.
55. *NIST Standard Reference Database*, 2003.
56. T. Ngu and M. J. Stillman, Metal-binding mechanisms in metallothioneins, *Dalton Transactions*, 2009, 5425-5433.
57. S. Toriumi, T. Saito, T. Hosokawa, T. Takashi, T. Numata and M. Kuraski, Metal binding ability of metallothionein-3 expressed in Escherichia coli, *Basic and Clinical Pharmacology & Toxicology*, 2005, **96**, 295-301.
58. N. Cols, N. Romero-Isart, M. Capdevila, B. Oliva, P. Gonzales-Duarte, R. Gonzales-Duarte and S. Atrian, Binding of excess Cd(II) to Cd7-metallothionein from recombinant mouse Zn7-metallothionein-1. UV-Vis absorption and Circular Dichroism studies and theoretical location approach by surface accessibility studies, *J. Inorg. Biochem.*, 1997, **68**, 157-166.
59. P. Palumaa, E. Eriste, O. Njunkova, L. Pokras, H. Jornvall and R. Sillard, Brain-specific metallothionein-3 has higher metal-binding capacity than ubiquitous metallothioneins and binds metals noncooperatively, *Biochemistry*, 2002, **41**, 6158-6163.
60. P. M. Gehrig, C. You, R. Dallinger, C. Gruber, M. Brouwer, J. R. Kagi and P. E. Hunziker, Electrospray ionization mass spectrometry of zinc, cadmium, and copper metallothioneins: Evidence for metal-binding cooperativity, *Protein Science*, 2000, **9**, 395-402.
61. L. T. Jensen, J. M. Peltier and D. T. Winge, Identification of a four copper folding intermediate in mammalian copper metallothionein by electrospray ionization mass spectrometry, *J. Bioinorg. Chem.*, 1998, **3**, 627-631.
62. M. P. Waallkes, M. J. Harvey and C. D. Klaassen, Relative in vitro affinity of hepatic metallothionein for metals, *Toxicology Letters*, 1984, **20**, 33-39.
63. J. Ejnik, J. Robinson, J. Zhu, H. Forsterling, C. F. I. Shaw and D. H. Petering, Folding pathway of apo-metallothionein induced by Zn(II), Cd(II), and Co(II), *J. Inorg. Biochem.*, 2002, **88**, 144-152.
64. M. J. Stillman, *Optical spectroscopy of metallothioneins. Metal-thiolate clusters in metallothioneins: Absorption, circular dichroism, magnetic circular dichroism, and emission spectra* Wiley-VCH, 1992.
65. T. T. Ngu and M. J. Stillman, Metalation of metallothioneins, *IUBMB Life*, 2009, **61**, 438-446.
66. G. W. Irvine, K. E. R. Duncan, M. Gullons and M. J. Stillman, Metalatin kinetics of the human alpha-metallothionein 1a fragment is dependent on the fluxional structure of the apo protein, *Chem. Eur. J.*, 2015, 1269-1279.
67. D. W. Hasler, L. T. Jensen, O. Zerbe, D. T. Winge and M. Vasak, Effect of the two conserved prolines of human growth inhibitory factor (metallothionein-3) on its biological activity and structure fluctuations: comparison with a mutant protein, *Biochemistry*, 2000, **39**, 14567-14575.
68. M. Erk and B. Raspor, *Anal. Chim. Acta.*, 1998, **360**, 189-194.
69. M. Vasak and J. H. R. Kagi, in *Metal Ions in Biological Systems*, ed. H. Sigel, 1982, vol. 15, pp. 213-273.
70. A. Muñoz and A. R. Rodríguez, Electrochemical behavior of metallothioneines and related molecules. Part III: Metallothionein, *Electroanalysis*, 1995, **7**, 674-680.
71. T. B. J. Pinter and M. J. Stillman, The Zinc Balance: Competitive Zinc Metalation of Carbonic Anhydrase and Metallothionein 1A, *Biochemistry*, 2014, **53**, 6276-6285.
72. D. Tekin, Z. Kayaalti and T. Soylemezoglu, The effects of metallothionein 2A polymorphism on lead metabolism: are pregnant women with a heterozycote genotype for metallothionein 2A polymorphism and their newborns at risk of having higher blood lead levels, *Int Arch Occup Environ Health*, 2012, **85**, 631-637.
73. S. M. Peterson, Z. Jun, G. Weber and J. L. Freeman, Global Gene Expression Analysis Reveals Dynamic and Developmental Stage–Dependent Enrichment of Lead-Induced Neurological Gene Alterations, *Environ. Health Persp.*, 2011, **119**, 615-621.
74. P. Zuo, R. N. Cooper, R. A. Goyer, B. A. Diwan and M. P. Waallkes, Potential role of alpha-synuclein and metallothionein in lead-induced inclusion body formation, *Toxicological sciences*, 2009, **111**, 100-108.
75. K.-I. Nakao, K. Kibayashi, T. Taki and H. Koyama, Changes in the Brain after Intracerebral Implanation of a Lead Pellet in the Rat, *J. Neurotraum*, 2010, **27**, 1925-1934.
76. D. Chu, Y. Tang, Y. Huan, W. He and W. Cao, The microcalorimetry study on the complexation of lead ion with metallothionein, *Thermochimica Acta*, 2000, **352-353**, 205-212.
77. Y. He, M. Lui, N. Darabedian, Y. Liang, D. Wu, J. Xiang and F. Zhou, pH-Dependent Coordination of Pb2+ to Metallothionein-2: Structures and Insight into Lead Detoxification, *Inorg. Chem.*, 2014, **53**, 2822-2830.
78. M. Salgado, K. L. Bacher and M. J. Stillman, Probing structural changes in the alpha and beta domains of copper- and silver-substituted metallothionein by emission spectroscopy and electrospray ionization mass spectrometry, *J. Biol. Inorg. Chem.*, 2007, **12**, 294-312.
79. O. Palacios, A. Leiva-Presa, S. Atrian and R. Lobinski, A study of the Pb(II) binding to recombinant mouse Zn7-metallothionein 1 and its domans by ESI TOF MS, *Talanta*, 2007, **72**, 480-488.
80. D. Wilcox, Isothermal titration calorimetry of metal ions binding to proteins: An overview of recent studies, *Inorganica Chimica Acta*, 2008, **361**, 857-867.
81. E. Chekmeneva, R. Prohens, J. M. Diaz-Crus, C. Arino and M. Esteban, Thermodynamics of Cd(II) and Zn(II) binding by the pytochelatin (gamma-Glu-Cys)4-Gly and its precursor glutathione, *Anal. Biochem.*, 2008, **375**, 82-89.
82. M. C. Carpenter and D. E. Wilcox, Thermodynamics of Formation of the Insulin Hexamer: Metal-stabilized Proton-Coupled Assembly of Quarternary Structure, *Biochemistry*, 2014, **53**, 1296-1301.
83. S. Leavitt and E. Freire, Direct measurement of protein binding energetics by isothermal titration calorimetry, *Curr Opin. Struct. Biol.*, 2001, **11**, 560-566.
84. H. Haase and W. Maret, Partial oxidation and oxidative polymerization of metallothionein, *Electrophoresis*, 2008, **29**, 4169-4176.
85. B. W. Sigurskjold, Exact analysis of competition ligand binding by displacement isothermal titration calorimetry, *Anal. Biochem.*, 2000, **277**, 260-266.
86. M. M. Pedroso, F. Ely, N. Mitić, L. R. Gahan, M. C. Carpenter, D. E. Wilcox, J. L. Larrabee, D. L. Ollis and G. Schenk, Comparative investigation of the reaction mechanisms of the organophosphate-degrading phosphotriesterases from Agrobacterium radiobacter (OpdA) and Pseudomonas diminuta (OPH), *J. Biol. Inorg. Chem.*, 2014, **19**, 1263-1275.
87. J. D. Otvos, D. H. Petering and C. F. Shaw, Structure-Reactivity Relationshpis of Metallothionein, a Unique Metal-Binding Protein, *Comments Inorg. Chem.*, 1989, **9**, 1-35.
88. M. A. Namdarghanbari, J. Meeusen, G. Bachowski, N. Giebel, J. Johnson and D. H. Petering, Reaction of the Zinc Sensor Fluo-Zin-3 with Zn7-metallothionein: Inquiry into the Existence of a Proposed Weak Binding Site, *J. Inorg. Biochem.*, 2010, **104**, 224-231.
89. M. Brouwer, in *Advances in Inorganic Biochemistry: mechanisms of metallocenter assembly*, eds. R. P. Hausinger, G. L. Eichhorn and L. G. Marzilli, 1996, vol. 11, pp. 235-260.
90. L. Banci, I. Bertini, S. Ciofi-Baffoni, T. Kozyreva, K. Zovo and P. Palumma, *Nature*, 2010, **465**, 645-650.

91. M. J. Lachenmann, J. E. Ladbury, J. Dong, K. Huang, P. Carey and M. A. Weiss, Why zinc fingers prefer zinc: Ligand-field symmetry and the hidden thermodynamics of metal ion selectivity, *Biochemistry*, 2004, **43**, 13910-13925.
92. A. M. Rich, E. Bombarda, A. D. Schenk, P. E. Lee, E. H. Cox, A. M. Spuches, L. D. Hudson, B. Keifer and D. E. Wilcox, Thermodynamics of Zn2+ Binding to Cys_2His_2 and $Cys_2HisCys$ Zinc Fingers and a Cys4 Transcription Factor Site, *J. Am. Chem. Soc.*, 2012, **134**, 10405-10418.
93. A. R. Reddi, T. R. Guzman, R. M. Breece, D. L. Tierney and B. R. Gibney, Deducing the Energetic Cost of Protein Folding in Zinc Finger Proteins Using Designed Metallopeptides, *J. Am. Chem. Soc.*, 2007, 12815-12827.
94. J. S. Magyar, T.-C. Weng, C. M. Stern, D. F. Dye, B. W. Rous, J. D. Payne, B. M. Bridgewater, A. Mijovilovish, G. Parkin, J. M. Zaleski, J. E. Penner-Hahn and H. A. Godwin, Reexamination of Lead(II) coordination preferences in sulfur-rich sites: Implications for a critical mechanism of lead poisoning, *J. Am. Chem. Soc.*, 2005, **127**, 9495-9505.
95. B. M. Bridgewater and G. Parkin, Lead poisoning and the inactivation of 5-aminolevulinate dehydratase as modeled by the tris(2-mercapto-1-phenylimidazolyl)hydroborato lead complex, {[TmPh]Pb}[ClO_4], *J. Am. Chem. Soc.*, 2000, **122**, 7140-7141.
96. T.-Y. Li, A. J. Kraker, C. F. I. Shaw and D. H. Petering, Ligand substitution reactions of metallothioneins with EDTA and apo-carbonic anhydrase, *Proc. Nat. Acad. Sci. USA*, 1980, **77**, 6334-6338.
97. G. W. Goldstein, Lead poisoning and brain cell function, *Environ. Health Persp.*, 1990, **89**, 91-94.
98. A. P. Neal and T. R. Guilarte, Molecular Neurobiology of Lead (Pb^{2+}): Effects on Synaptic Function, *Mol Neurobiol*, 2010, **42**, 151–160.
99. J. Ejnik, A. Munoz, T. Gan, C. F. Shaw and D. H. Petering, Interprotein metal ion exchange between cadmium-carbonic anhydrase and apo- or zinc-metallothionein, *JBIC*, 1999, **4**, 784-790.
100. A. Karotki and M. Vasak, Reaction of human metallothionein-3 with cisplatin and transplatin, *J. Biol. Inorg. Chem.*, 2009, **14**, 1129-1138.

